

## Observation of Laser-Induced Melting of Silicon Film Followed by Amorphization

Toshiyuki SAMESHIMA, Masaki HARA, Naoki SANO  
and Setsuo USUI

*Sony Research Center, 174 Fujitsuka-cho, Hodogaya-ku, Yokohama 240*

(Received April 11, 1990; accepted for publication July 5, 1990)

Transient conductance measurements were used to study laser-induced amorphization of polycrystalline silicon (poly-Si) film. A 20 nm-thick phosphorus-doped poly-Si film fabricated on a quartz substrate was melted by irradiation with a 30 ns-pulsed XeCl excimer laser. When the melt duration exceeded 70 ns, the silicon film was completely amorphized through rapid solidification. Formation of the amorphous thin film may be brought about by homogeneous solidification without crystalline nucleation.

**KEYWORDS:** laser-induced amorphization, laser-induced crystallization

### §1. Introduction

Pulsed laser-induced melt-regrowth has been studied by many researchers to clarify phenomena such as the crystallization of amorphous silicon and the amorphization of crystalline silicon.<sup>1-8)</sup> Surface amorphization of silicon has been achieved using short laser pulses (< 10 ns), in particular with a short wavelength (UV-VIS), because rapid solidification with a large regrowth velocity of > 15 m/s is required.<sup>4-8)</sup> Surface amorphization is initiated with a laser energy density just above the melting threshold. The molten silicon layer, however, returns to the crystalline state with a laser energy density greater than the amorphizing threshold because the regrowth velocity decreases.<sup>8)</sup>

On the other hand, we have reported that a thin polycrystalline silicon (poly-Si) film fabricated on a quartz substrate was amorphized by irradiation using a XeCl excimer laser with a long pulse of 30 ns (FWHM).<sup>9)</sup> Nondoped and phosphorus-doped poly-Si films were completely amorphized with a laser energy density much larger than the melting threshold. The molten silicon returned to the crystalline state with laser energy densities below the amorphizing threshold. The mechanism of the complete amorphization of the silicon films, however, is not yet clear.

This work reports the investigation on the melt-regrowth characteristics of a poly-Si film using a transient conductance technique in order to study the mechanism of the amorphization of silicon films.

### §2. Transient Conductance Measurements

Figure 1 shows a schematic diagram of the apparatus used for transient conductance measurements. A 20 nm-thick phosphorus-doped hydrogenated amorphous silicon (a-Si:H, P) film was deposited on a quartz substrate at 250°C using a radio-frequency glow discharge (rf-GD). Then, 50 SCCM SiH<sub>4</sub> (10%)/Ar and 10 SCCM PH<sub>3</sub> (1%)/Ar mixed with 50 SCCM H<sub>2</sub> gas was decomposed. The a-Si:H, P film was patterned into 1 mm-wide stripes and aluminium electrodes with a gap of 1 mm and width of 3 mm were formed on the stripes.

The sample was then connected to a load resistance of 50ohms and a bias voltage was applied. Irradiation was provided by a 30 ns-pulsed XeCl excimer laser ( $\lambda = 308$  nm) in air at room temperature. The sample was irradiated with a laser beam whose spot size was focused through a lens to 5 mm  $\times$  10 mm. The transient current during and after irradiation was measured across the load resistance by a high-speed storage oscilloscope. The melting threshold energy (= 130 mJ/cm<sup>2</sup>) was determined by time-resolved optical reflectivity measurements using an Ar-514.5 nm laser beam as a probe light.<sup>10)</sup>

Laser-induced amorphization and crystallization were distinguished by the conductance of the sample after solidification because the conductance for phosphorus-doped (P-doped) laser amorphous silicon ( $\sim 10^{-1}$  S/cm) is much smaller than that for P-doped poly-Si ( $\sim 10^3$  S/cm).<sup>9)</sup> Amorphization and crystallization could also be observed visually because the 20 nm-thick amorphous silicon film is dark brown while the poly-Si film is yellowish brown.

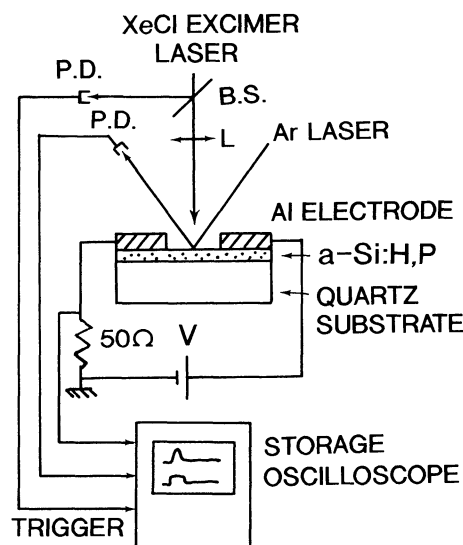


Fig. 1. Schematic diagram of measurement apparatus for transient conductance and time-resolved optical reflectivity.

### §3. Results and Discussion

Figure 2 shows the evolution of transient conductance during and after irradiation with 5 pulses. The a-Si:H, P film was melted and crystallized by irradiation with the first pulse at an energy density of  $215 \text{ mJ/cm}^2$ . The conductance associated with molten silicon appeared first. It increased to  $0.008 \text{ S}/\square$  and then gradually decreased, as shown in curve A of Fig. 2(a). After the termination of the melt, there was a large residual conductance in the P-doped Si film. The conductivity was  $1.7 \times 10^3 \text{ S/cm}$  at room temperature after the irradiation, although the conductivity of the as-deposited a-Si:H, P film was  $1 \times 10^{-3} \text{ S/cm}$ . The increase of conductivity with irradiation was brought about by an increase in carrier mobility and activation ratio.<sup>11)</sup> The sample was also melted and recrystallized by irradiation with a second pulse at an energy density of  $235 \text{ mJ/cm}^2$ . The conductance in the molten region was larger than that brought about by irradiation with the first pulse, as is shown in curve B of Fig. 2(a). This shows that the sample was melted deeper by the irradiation. Transmission electron micrography and optical reflectivity measurements have revealed that the silicon film is completely crystallized by irradiation at both energies,<sup>12,13)</sup> although the film was not completely melted. Lowndes *et al.* reported that amorphous silicon below the molten layer is crystallized through the explosive propagation of a buried molten layer and a fine

grain layer is formed.<sup>14)</sup> Although we guess that Lowndes *et al.*'s explosive crystallization can be applied to the crystallization of a-Si:H, the mechanism for the complete crystallization of a-Si:H is not yet clear.

The sample was then melted by irradiation with a third pulse at an energy density of  $245 \text{ mJ/cm}^2$ . The conductance in molten silicon rapidly increased and then rapidly decreased at  $85 \text{ ns}$  after the initiation of melt from 75% to 6% of the maximum conductance within  $5 \text{ ns}$  (=time resolution), as is shown in Fig. 2(b). After solidification, the conductance decreased below the noise level of  $1 \times 10^{-5} \text{ S}/\square$ . This decrease of conductance after solidification means that the P-doped poly-Si film was completely melted and completely amorphized. The conductance in molten silicon changed gradually near the maximum conductance, as can be seen in Fig. 2(b). This is probably caused by the reduction of the melt depth near the edges of the Al electrodes because of lateral heat diffusion. The transition from amorphous to liquid to amorphous occurred with irradiation with a fourth pulse at  $245 \text{ mJ/cm}^2$ . The peak conductance in the molten region was smaller than that caused by irradiation with the third pulse. This is probably because of a pulse-to-pulse fluctuation in laser energy of  $\pm 5\%$ . Rapid solidification occurred  $70 \text{ ns}$  after the initiation of melt, as shown in Fig. 2(c). The change in conductance of the molten silicon is similar to the change in conductance caused by irradiation with the third pulse, as can be seen in Fig. 2(b). The conductance

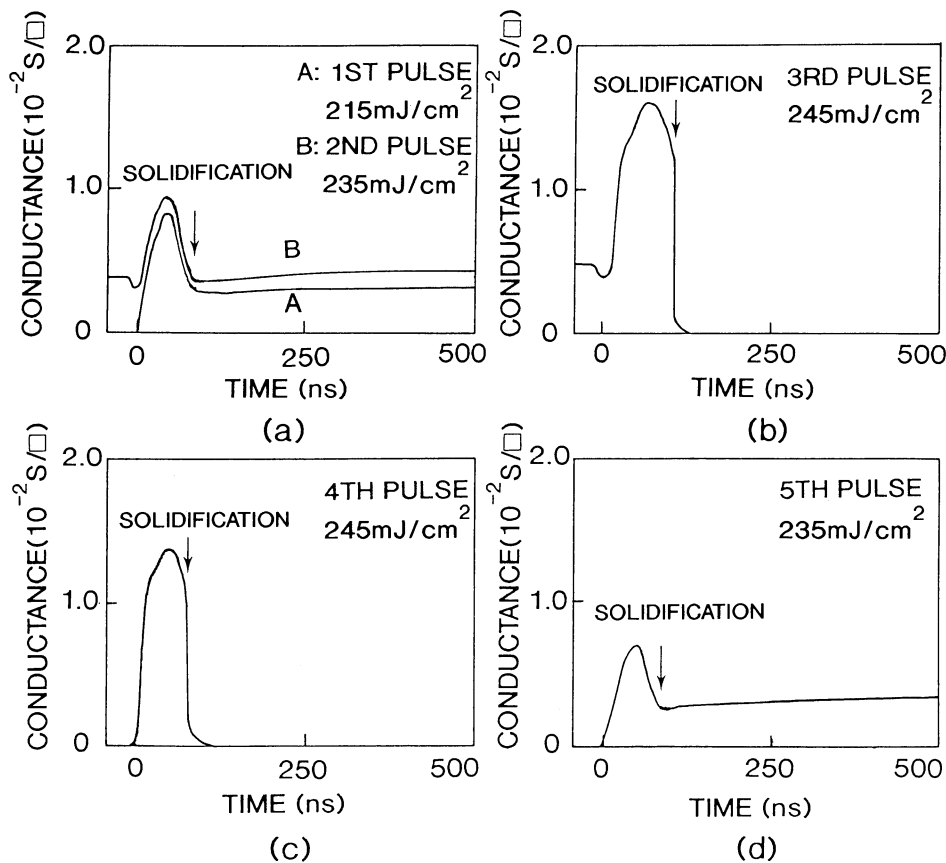


Fig. 2. Conductance of 20 nm-thick P-doped silicon film as a function of time with irradiation with five pulses; energy density was  $215 \text{ mJ/cm}^2$  for curve A in (a),  $235 \text{ mJ/cm}^2$  for curve B in (a),  $245 \text{ mJ/cm}^2$  in (b),  $245 \text{ mJ/cm}^2$  in (c) and  $235 \text{ mJ/cm}^2$  in (d).

after solidification was still smaller than the noise level. The sample was then recrystallized by the irradiation with a fifth pulse at  $235 \text{ mJ/cm}^2$ , as shown in Fig. 2(d). The conductivity in the P-doped silicon film increased to  $1.8 \times 10^3 \text{ S/cm}$  after solidification.

Transient conductance measurements revealed that the molten silicon on the quartz substrate was rapidly solidified and completely amorphized when the peak conductance in molten silicon and the melt duration exceeded  $0.0013 \text{ S/}\square$  and  $70 \text{ ns}$  at half-maximum of the conductance in molten silicon, respectively. Up to the thresholds, molten silicon was gradually solidified and crystallization occurred. We deduce that the laser-induced amorphization occurs through homogeneous solidification because the temperature could distribute uniformly in molten silicon during a long melt duration.

The temperature gradient in molten silicon was simply estimated using the unidimensional heat diffusion equation. It was assumed that the  $20 \text{ nm}$ -thick silicon film was completely melted by irradiation with a pulse which has a square shape with a width of  $30 \text{ ns}$ . The heat diffusion in molten silicon with two boundaries—air/liquid silicon/quartz—was analyzed by mean of the imaging method.<sup>15</sup> We used the values of thermal conductivity and specific heat in molten silicon deduced by Wood and Giles<sup>16</sup> and those in quartz from a compilation of the values of Goldsmith *et al.*<sup>17</sup> The calculated temperature gradient in molten silicon was  $2.2 \times 10^5 \text{ K/cm}$  ( $\sim 0.4 \text{ K/20 nm}$ ) at the interface between silicon and quartz substrate at  $70 \text{ ns}$  after the initiation of melt when molten silicon supercools to  $1350 \text{ K}$ <sup>18</sup> to form amorphous silicon. Thus, the temperature was uniformly distributed in the molten silicon layer at  $70 \text{ ns}$  after the initiation of melt. This indicates that the supercooled molten silicon can be solidified rapidly and homogeneously throughout the film. Stiffler *et al.*, however, reported that supercooled molten silicon was not amorphized but crystallized through homogeneous solidification when a  $300 \text{ nm}$ -thick zone-melted recrystallized silicon film was melted by a pulsed ruby laser.<sup>3</sup> The reason why the amorphization occurs only in thin film is not clear at present. Research on that mechanism is in progress.

Below the threshold melt duration of  $70 \text{ ns}$ , crystallization of the silicon film occurs, probably through the interface-controlled growth of molten silicon<sup>18</sup> because there can be a large temperature gradient in the molten region when the melt duration is short.

## §5. Conclusions

The characteristics of melt and regrowth on  $20 \text{ nm}$ -thick phosphorus-doped silicon film deposited on the quartz substrate were investigated. Molten silicon was crystallized by irradiation with a  $30 \text{ ns}$ -pulsed XeCl excimer laser when the melt duration is up to  $70 \text{ ns}$  at half-maximum of conductance in the molten region. Molten

silicon was rapidly solidified and the film was amorphized when the melt duration was above  $70 \text{ ns}$ . Complete amorphization means that the silicon film was completely melted. Because molten silicon has almost the same temperature throughout the film thickness after  $70 \text{ ns}$ , the thin molten layer on the quartz may be solidified homogeneously without crystalline silicon nucleation.

## Acknowledgements

We would like to thank Dr. M. Hirose, Dr. M. Kikuchi and Dr. Y. Kawana for the helpful discussions and M. Nakagoe, M. Kamada and K. Kunisada for their experimental support. We also wish to acknowledge the support of Dr. S. Watanabe.

## References

- 1) R. F. Wood, D. H. Lowndes and J. Narayan: *Appl. Phys. Lett.* **44** (1984) 770.
- 2) M. O. Thompson, G. J. Galvin, J. W. Mayer, P. S. Peercy, J. M. Poate, D. C. Jacobson, A. G. Cullis and N. G. Chew: *Phys. Rev. Lett.* **52** (1984) 2360.
- 3) S. R. Stiffler, M. O. Thompson and P. S. Peercy: *Proc. MRS (1988) on Fundamentals of Beam-Solid Interaction and Transient Thermal Processing*, eds. M. J. Aziz, L. E. Rehn and B. Stritker (Material Research Society, Pittsburgh, 1988) p. 505.
- 4) P. L. Liu, R. Yen, N. Bloembergen and R. T. Hodgson: *Appl. Phys. Lett.* **34** (1979) 864.
- 5) R. Tu, R. T. Hodgson, T. Y. Tan and J. E. Baglin: *Phys. Rev. Lett.* **42** (1979) 1356.
- 6) A. G. Cullis, H. C. Webber, N. G. Chew, J. M. Poate and P. Baeri: *Phys. Rev. Lett.* **49** (1982) 219.
- 7) S. U. Campisano, D. C. Jacobson, J. M. Poate, A. G. Cullis and N. G. Chew: *Appl. Phys. Lett.* **46** (1985) 846.
- 8) M. O. Thompson, J. W. Mayer, A. G. Cullis, H. C. Webber, N. G. Chew, J. M. Poate and D. C. Jacobson: *Phys. Rev. Lett.* **50** (1983) 896.
- 9) T. Sameshima, M. Hara and S. Usui: *Jpn. J. Appl. Phys.* **29** (1990) 548.
- 10) D. H. Auston, J. A. Golovchenko, P. R. Smith, C. M. Surko and T. N. C. Venkatesan: *Appl. Phys. Lett.* **33** (1978) 538.
- 11) T. Sameshima, M. Hara and S. Usui: to be published in *Proc. MRS (1989) on In-situ Patterning: Selective Area Deposition and Etching Processing*, eds. A. F. Bernhardt, R. Rosenberg and J. G. Black (Material Research Society, Pittsburgh, 1989).
- 12) T. Sameshima, M. Hara and S. Usui: *Jpn. J. Appl. Phys.* **28** (1989) 1789.
- 13) T. Sameshima, M. Hara and S. Usui: *Proc. MRS (1986) on Materials Issues in Silicon Integrated Circuit Proceedings*, eds. M. Wittmer, J. Stimmell and M. Strathmann (Material Research Society, Pittsburgh, 1989) p. 435.
- 14) D. H. Lowndes, G. E. Jellison, Jr., S. J. Pennycook, S. P. Withrow and D. N. Mashburn: *Appl. Phys. Lett.* **48** (1986) 1389.
- 15) H. S. Carslaw and J. C. Jager: *Conduction of Heat in Solids* (Oxford University Press, Oxford, 1959) Chap. 2.
- 16) R. F. Woods and G. E. Giles: *Phys. Rev.* **B23** (1981) 2923.
- 17) A. Goldsmith, T. E. Waterman and H. J. Hirschhorn: *Handbook of Thermophysical Properties of Solid Materials* (Pergamon, New York, 1961) Vol. 1.
- 18) F. Spaepen and D. Turnbull: *Laser Annealing of Semiconductors*, eds. J. Poate and J. W. Mayer (Academic, New York, 1982) Chap. 2.